THE STRUCTURE AND DYNAMICS OF MASSIVE EARLY-TYPE GALAXIES

Koopmans, L. V. E.; Bolton, A.; Treu, T.; Czoske, O.; Auger, M. W.; Barnabe, M.; Vegetti, S.; Gavazzi, R.; Moustakas, L. A.; Burles, S.

Published in:
Astrophysical Journal Letters

DOI:
10.1088/0004-637X/703/1/L51

Publication date:
2009

The Astrophysical Journal, 703:L51–L54, 2009 September 20 doi:10.1088/0004-637X/703/1/L51

THE STRUCTURE AND DYNAMICS OF MASSIVE EARLY-TYPE GALAXIES: ON HOMOLOGY, ISOTHERMALITY, AND ISOTROPY INSIDE ONE EFFECTIVE RADIUS

L. V. E. Koopmans[1], A. Bolton[2], T. Treu[3], O. Czoske[1], M. W. Auger[3], M. Barnabè[1], S. Vegetti[1], R. Gavazzi[4], L. A. Moustakas[5], and S. Burles[6]

[1] Kapteyn Astronomical Institute, University of Groningen, P.O.Box 800, 9700 AV Groningen, The Netherlands; koopmans@astro.rug.nl
[2] Institute for Astronomy, University of Hawaii, 2680 Woodlawn Dr., Honolulu, HI 96822, USA; bolton@ifa.hawaii.edu
[3] Department of Physics, University of California, Santa Barbara, CA 93106, USA; ttreu@physics.ucsb.edu
[4] Institut d'Astrophysique de Paris, UMR7095 CNRS - Université Paris 6, 98bis Bd Arago, 75014 Paris, France; gavazzi@iap.fr
[5] JPL/Caltech, MS 169-327, 4800 Oak Grove Dr., Pasadena, CA 91109, USA; leonidas@jpl.nasa.gov
[6] Department of Physics and Kavli Institute for Astrophysics and Space Research, Massachusetts Institute of Technology, 77 Massachusetts Avenue, Cambridge, MA 02139, USA; burles@mit.edu

Received 2009 June 10; accepted 2009 August 12; published 2009 September 2

ABSTRACT

Based on 58 SLACS strong-lens early-type galaxies (ETGs) with direct total-mass and stellar-velocity dispersion measurements, we find that inside one effective radius massive elliptical galaxies with $M_{\rm eff} \gtrsim 3 \times 10^{10}\,M_{\odot}$ are well approximated by a power-law ellipsoid, with an average logarithmic density slope of $\langle \gamma'_{\rm LD} \rangle \equiv -d\log(\rho_{\rm tot})/d\log(r) = 2.085^{+0.025}_{-0.018}$ (random error on mean) for isotropic orbits with $\beta_r = 0, \pm 0.1$ (syst.) and $\sigma_{\gamma'} \lesssim 0.20^{+0.04}_{-0.02}$ intrinsic scatter (all errors indicate the 68% CL). We find no correlation of $\gamma'_{\rm LD}$ with galaxy mass ($M_{\rm eff}$), rescaled radius (i.e., $R_{\rm einst}/R_{\rm eff}$) or redshift, despite intrinsic differences in density-slope between galaxies. Based on scaling relations, the average logarithmic density slope can be derived in an alternative manner, fully independent from dynamics, yielding $\langle \gamma'_{\rm SR} \rangle = 1.959 \pm 0.077$. Agreement between the two values is reached for $\langle \beta_r \rangle = 0.45 \pm 0.25$, consistent with mild radial anisotropy. This agreement supports the robustness of our results, despite the increase in mass-to-light ratio with total galaxy mass: $M_{\rm eff} \propto L_{V,{\rm eff}}^{1.363\pm0.056}$. We conclude that massive ETGs are structurally close to homologous with close to isothermal total density profiles ($\lesssim$10% intrinsic scatter) and have at most some mild radial anisotropy. Our results provide new observational limits on galaxy formation and evolution scenarios, covering 4 Gyr look-back time.

Key words: galaxies: structure – gravitational lensing

1. INTRODUCTION

Understanding the internal structure of massive early-type galaxies (ETGs) is essential if we ever hope to fully understand hierarchical galaxy formation (e.g., Davis et al. 1985; Frenk et al. 1985; White & Frenk 1991) and the complex interplay between dark matter and baryons. A number of tight relations, such as the fundamental plane (FP hereafter; Dressler et al. 1987; Djorgovski & Davis 1987), the color–magnitude relation (e.g., Visvanathan & Sandage 1977; Sandage & Visvanathan 1978; Bower et al. 1992), and the relation between black-hole and stellar spheroid masses (Kormendy & Richstone 1995; Magorrian et al. 1998; Ferrarese & Merritt 2000; Gebhardt et al. 2000), indicate that there must be physical processes that are not dominated by stochastic processes of hierarchical galaxy formation.

In the FP relation of ETGs both stars and dark matter contribute to the structure and dynamics ($\sigma_{\rm c}$) and total mass-to-light ratio (M/L). Hence, without knowledge of the dark-matter distribution and stellar populations, we remain clueless about whether changes in the FP are due to non-homology or due to changes in their stellar mass-to-light, or both (e.g., Hjorth & Madsen 1995; Prugniel & Simien 1997; Treu et al. 1999; Gerhard et al. 2001; Bertin et al. 2002; Cappellari et al. 2006; Nipoti et al. 2006; Graves et al. 2009). Given only first and second moments of the stellar velocity distribution, disentangling these effects has remained difficult because of the mass-anisotropy degeneracy: steepening of the density profile and changes in the orbital anisotropy can offset each other to yield similar kinematic profiles (e.g., Gerhard 1993; Gerhard et al. 1998; Łokas & Mamon 2003). In studying the tilt of the FP (e.g., Renzini & Ciotti 1993), one can therefore not easily disentangle effects of mass structure (e.g., non-homology) from changes in stellar mass-to-light ratios, using only stellar kinematics.

In recent papers (Bolton et al. 2006; Treu et al. 2006; Koopmans et al. 2006; Bolton et al. 2007; Gavazzi et al. 2007; Bolton et al. 2008a), we analyzed a subsample of well-selected gravitational lens systems from the SLACS Survey,[7] showing that massive elliptical galaxies have on average close to isothermal density profiles, with some minor, but noticeable, intrinsic scatter between their logarithmic density slopes (e.g., Koopmans et al. 2006; Treu & Koopmans 2004). They follow the classical FP (Treu et al. 2006), as well as a tight mass fundamental plane (MFP; Bolton et al. 2007, 2008b), where galaxy surface brightness is replaced by surface density. In all observable respects, they follow the trends of normal elliptical galaxies (Bolton et al. 2006; Treu et al. 2006; Bolton et al. 2008a; Treu et al. 2009) and these lens-based results can thus be extended to non-lens galaxies in the same parameter space (e.g., Hyde & Bernardi 2009; Mandelbaum et al. 2009).

In this Letter we study the total mass-density profile of massive ETGs inside one effective radius, using the *full* SLACS sample of 58 gravitational lens systems with high-fidelity *Hubble Space Telescope*/Advanced Camera for Surveys (*HST*/ACS) observations. We examine the intrinsic scatter in density slopes that is allowed by the sample, whether the slope correlates with other global parameters and we set limits on the level of

[7] http://www.slacs.org

orbital anisotropy in these systems. In Section 2, we present the logarithmic density slopes of the SLACS early-type lens galaxies, based on two different methods, one based on lensing and dynamics and one based on scaling relations, that explicitly include their average density profile as a free parameter. Comparing these two values allows us to set limits on their average orbital anisotropy. In Section 3, we summarize our results and conclusions. Throughout this Letter, we make use of the sample of 58 SLACS single-lens systems from Bolton et al. (2008a) and take all quantities from that paper. If not mentioned otherwise, all masses are in units of $10^{10}\,M_{\odot}$. We assume $\Omega_{\rm m} = 0.3$, $\Omega_{\Lambda} = 0.7$, and $H_0 = 100\,h$ km s^{-1} Mpc^{-1}.

2. THE DENSITY PROFILE OF MASSIVE ETGs

To determine the logarithmic slope of the total density profile, we use two alternative methods: (1) through combining SDSS-based stellar velocity dispersions and lensing-based total masses, and (2) through scaling relations between luminosity, mass, and rescaled radius, which does *not* require a measured stellar velocity dispersion. Whereas a single power law mass model is an approximation, Koopmans & Treu (2003), Treu & Koopmans (2004), and Barnabè et al. (2009) show that two-component models can robustly be approximated by a single power-law component given current data quality.

2.1. Derivation from Lensing and Stellar Dynamics

To derive the logarithmic density slopes, we follow Treu & Koopmans (2002), Koopmans & Treu (2003), Treu & Koopmans (2004), and Koopmans et al. (2006). First the lensing mass inside the critical curves is determined from the lens models in Bolton et al. (2008a), which is nearly invariant under changes in the density profile (Kochanek 1991), hence the assumed density profile during this step is not relevant in further steps (see Koopmans et al. 2006). Subsequently we solve the spherical Jeans equations—assuming this mass as external constraint and an Einstein radius equal to the deflection angle of an equivalent spherical mass distribution—for a luminosity-density profile that follows either a Hernquist (1990) or Jaffe (1983) profile, embedded as trace-component inside the total density profile $\rho_{\rm tot} \propto r^{-\gamma'_{\rm LD}}$ (i.e., a power-law profile). The half-light radius of the projected luminosity-density profile is set equal to the observed effective radius (Bolton et al. 2008a). We take seeing (FWHM = 1.5 arcsec) into account. We vary the slope $\gamma'_{\rm LD}$ over a range of 1.1–2.9 and compare the predicted velocity dispersion inside the 3 arcsec diameter SDSS fiber with the observed value. The error in the measured velocity dispersion is by far the most dominant source of uncertainty. Hence, the likelihood $dP/d\gamma'_{\rm LD} \propto e^{-\chi^2/2}$ is determined from the χ^2 mismatch between the model and observed velocity-dispersion values.

The results in Figure 1 show that most values lie around a slope of 2, which is that of an isothermal mass profile ($\rho \propto r^{-2}$). A joint analysis of the sample yields

$$\langle \gamma'_{\rm LD} \rangle \equiv -d\log(\rho_{\rm tot})/d\log(r) = 2.085^{+0.025}_{-0.018}(68\%{\rm CL}), \quad (1)$$

in the range of radii 0.2–1.3 $R_{\rm eff}$ and for $\beta_r = 0$. The dependence on orbital anisotropy is small with the slopes varying mildly over $\beta_r = \pm 0.50$ (see Figure 1). Based on changing the luminosity density profile, seeing, etc., we estimate an $\sim$0.1 systematic error. We note two points: (1) a more detailed two-dimensional kinematic analyses of six SLACS galaxies (see Czoske et al. 2008; Barnabè et al. 2009) agree with these results, and (2) comparing the density slopes of the 14 systems that overlap with Koopmans et al. (2006), we find an average increase of $\gamma'_{\rm LD}$ by 6%. This difference can be attributed to minor model improvements, the use of better *HST* images, leading to an average decrease of $R_{\rm eff}$ by 13%, and an improved derivation of the stellar velocity dispersion, leading to an increase by +3%. In particular, the latter leads to an average increase in $\gamma'_{\rm LD}$, explaining most of the difference. Hence currently we are limited by systematics.

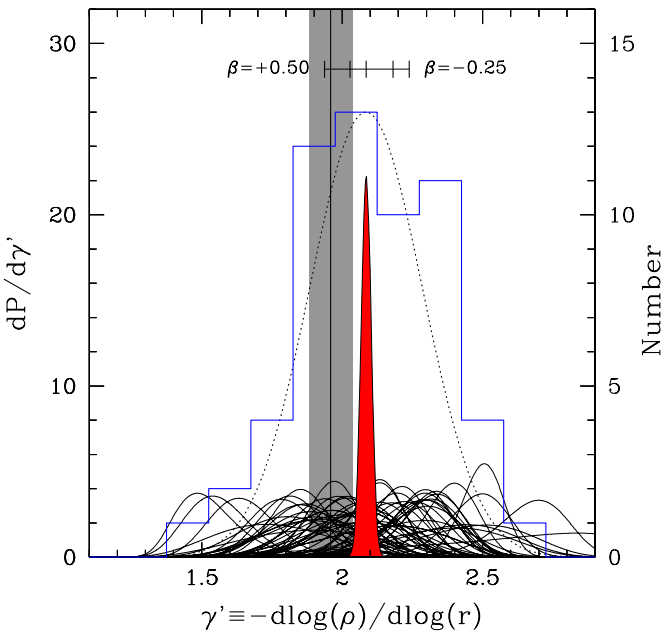

Figure 1. Logarithmic density slopes of 58 SLACS ETGs (thin solid curves). The filled red curve is the joint likelihood of the *ensemble-average* density slope. The histogram indicates the distribution of median values and the dotted Gaussian curve indicates the intrinsic scatter in $\gamma'_{\rm LD}$ (see text for details). We assume a Hernquist luminosity-density profile. The small dashes indicate the shift in the ensemble-average density slope for $\beta_r = +0.50, +0.25, -0.50, -0.25$ (left to right), respectively. Note the reversal of the $\beta_r = -0.50$ and -0.25 dashes. The vertical solid line and gray region indicate the best-fit value and 68% CL interval, respectively, of the average density derived from scaling relations.

An intrinsic spread of $\sigma_{\gamma'} = 0.20^{+0.04}_{-0.02}$ (i.e., $\sigma_{\gamma'}/\langle\gamma'_{\rm LD}\rangle = 0.10^{+0.02}_{-0.01}$; 68% CL) is derived, assuming Gaussian intrinsic and error distributions (see Koopmans et al. 2006; Barnabè et al. 2009) consistent with the scatter found in Koopmans et al. (2006), Jiang & Kochanek (2007), and Barnabè et al. (2009). Despite the uniformity of the sample, differences between galaxies are present, which could partly be physical (see, e.g., Gerhard et al. 2001), partly due to systematics, or due to small uncorrelated contributions from the environment and large-scale structure (Auger 2008; Treu et al. 2009; Guimarães & Sodré 2009). Conservatively it should therefore be regarded as an upper limit on *physical* variations.

2.2. Derivation from Scaling Relations

A second method to derive the ensemble-average density profile is to assume a scaling relation between the observables, luminosity, effective radius, and Einstein radius and Einstein mass:

$$\alpha \log(L_{\rm eff}) = \log\left[M_{\rm einst}\left(\frac{R_{\rm eff}}{R_{\rm einst}}\right)^{(3-\gamma'_{\rm SR})}\right] + \delta. \quad (2)$$

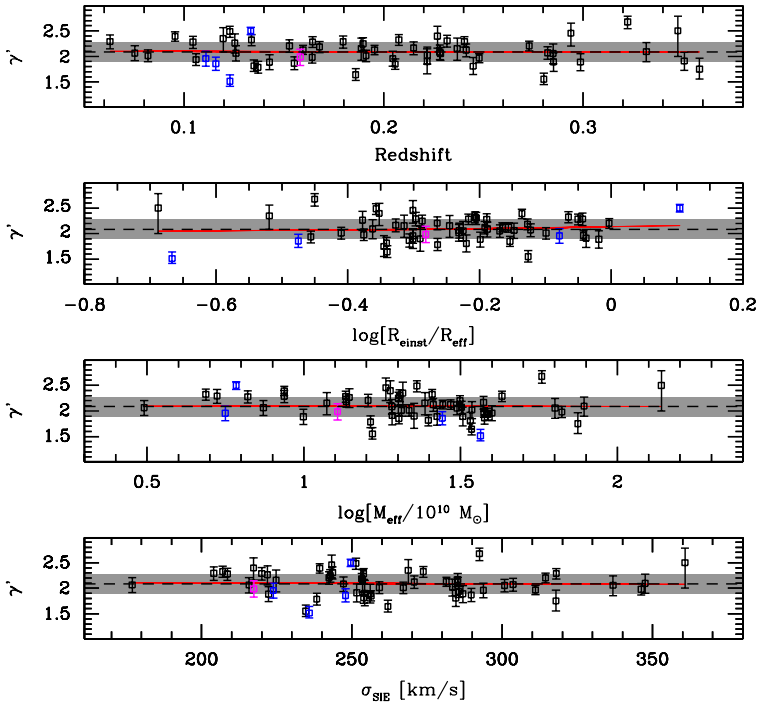

Figure 2. Median values of $\gamma'_{\rm LD}$ versus global galaxy quantities and redshift. The blue symbols are S0 galaxies and the magenta colored system is an E/S0 galaxy. The dashed curves are given at $\gamma'_{\rm LD} \equiv 2.085$ for reference with the gray box being $\pm 10\%$ intrinsic scatter. The thin red line is the best linear fit (i.e., shown curved in the log-plots).

This relation assumes that the density profile scales as a power law with $\rho \propto r^{-\gamma'_{\rm SR}}$ and that mass and light scale with $M_{\rm eff} \propto L_{\rm eff}^{\alpha}$ with $M_{\rm eff} \equiv M_{\rm einst}\,(R_{\rm eff}/R_{\rm einst})^{(3-\gamma'_{\rm SR})}$. The idea is that for a fixed luminosity, $M_{\rm einst}$ scales with $R_{\rm einst}/R_{\rm eff}$ and thus provides an ensemble-averaged density slope.

This approach is slightly different from Bolton et al. (2008a), who assumed a SIE or constant M/L mass profile in deriving the MFP, but similar to Rusin & Kochanek (2005) who focused on the FP and density slope. It allows us to derive the density slope *independently* from assumptions about stellar dynamics. The resulting values are $\alpha = 1.363 \pm 0.056$, $\delta = -0.959 \pm 0.050$ and for the best-fit ensemble-average logarithmic density slope

$$\langle \gamma'_{\rm SR} \rangle = 1.959 \pm 0.077. \quad (3)$$

This result is close to that derived based on dynamics models, although it assumes nothing about the dynamical structure of these galaxies (e.g., isotropy). The value of $\alpha \equiv 1/\eta'$, with η' as defined and given in Bolton et al. (2008a). The difference between $\langle \gamma'_{\rm SR} \rangle$ and $\langle \gamma'_{\rm LD} \rangle$ of $\sim$0.1 implies that on average anisotropy cannot be very large (see Section 2.4).

2.3. Correlations of Slope and Galaxy Properties

To assess whether $\gamma'_{\rm LD}$ correlates with global galaxy quantities or cosmic time, we plot them against effective mass, rescaled $(R_{\rm einst}/R_{\rm eff})$ radius, and redshift. The results are shown in Figure 2. We find the following linear gradients:

$$\begin{cases} d\gamma'_{\rm LD}/d\sigma_{\rm SIE} = (-1.6 \pm 8.3) \times 10^{-4} \\ d\gamma'_{\rm LD}/dM_{\rm eff} = (-0.6 \pm 14.5) \times 10^{-4} \\ d\gamma'_{\rm LD}/d(R_{\rm einst}/R_{\rm eff}) = (0.10 \pm 0.16) \\ d\gamma'_{\rm LD}/dz = (-0.05 \pm 0.43), \end{cases} \quad (4)$$

with $\sigma_{\rm SIE}$ in units of km s^{-1} and $M_{\rm eff}$ in units of $10^{10}\,M_{\odot}$. No weights on the points are used to avoid the brighter low-redshift galaxies from dominating the fits. We find no correlations at any significant level. Similar results were found by Koopmans et al. (2006) and recently by Auger (2008), Treu et al. (2009), and Guimarães & Sodré (2009), based on studies of their environment and mass along the line of sight. Overall, the inner regions ($R \lesssim R_{\rm eff}$) of massive early-type ($>L_*$) galaxies are remarkably homologous and simple. This result is unlike some of the more detailed results found by the SAURON collaboration for $\lesssim L_*$ galaxies (e.g., Cappellari et al. 2006; Emsellem et al. 2007), which show a range of different kinematic signatures (e.g., counter-rotating cores, triaxiality, fast versus slow rotators, etc.). We find that these complexities, at least at the high-mass end, do not seem to affect the derivation of their mass distributions and scaling relations (see, e.g., Barnabè et al. 2009, for a discussion), although the overlap between the samples in mass is small. The analyses of six SLACS lens systems (Czoske et al. 2008; Barnabè et al. 2009), based on VLT VIMOS-IFU data, shows that the majority of the SLACS galaxies are slow rotators predominantly supported by random stellar motions.

2.4. Limits on Orbital Anisotropy

Of the two methods to derive the average density slope, one depends on dynamics and the other does not. In the former, we assumed $\beta_r = 0$. If the galaxies, however, on average have a different value of β_r, the average value of $\gamma'_{\rm LD}$ can be either too large or too small, since we would attribute a higher/lower dispersion to a steeper/shallower density slope and not to radial/tangential orbital anisotropy.

The independence of the second method from dynamics allows us therefore to place constraints on the average orbital anisotropy of the ensemble of galaxies $\langle \beta_r \rangle$. As indicated in Figure 1, good agreement is found for a positive value of $\langle \beta_r \rangle \approx 0.45 \pm 0.25$, in agreement with results from Gerhard

et al. (2001). The galaxies are at most mildly radial anisotropic, as also found in Czoske et al. (2008) and Barnabè et al. (2009) from a more detailed two-integral and two-dimensional analysis of SLACS systems.

3. RESULTS AND CONCLUSIONS

We have presented a complete analysis of the inner mass density profile of 58 ETGs from the SLACS survey, focusing on their logarithmic density slope. We find the following results for galaxies with $M_{\rm eff} \gtrsim 3 \times 10^{10}\,M_{\odot}$:

1. Based on lensing and stellar dynamics constraints, the *average* inner logarithmic density slope in their inner 0.2–1.3 $R_{\rm eff}$ is $\langle\gamma'_{\rm LD}\rangle = 2.085^{+0.025}_{-0.018}$ (random error on mean; 68% CL; for isotropic orbits, $\beta_r = 0$), ±0.1 (syst.) and a small ($\lesssim$0.1) dependence on anisotropy for a range of $\beta_r = \pm0.50$. An intrinsic scatter in $\gamma'_{\rm LD}$, between individual galaxies, of $\sigma_{\gamma'} \lesssim 0.20^{+0.04}_{-0.02}$ (68% CL) is still allowed by our data. This should be regarded as an upper limit on physical variations, since it must include residual systematic effects. However, we believe part of it to be due to real differences between ETG density profile slopes (see also Barnabè et al. 2009).
2. A second independently derived value of the *average* inner logarithmic density slope is found from scaling relations, yielding $\langle\gamma'_{\rm SR}\rangle = 1.959 \pm 0.077$. This value is completely independent from dynamics and therefore a robust sanity check of the lensing plus dynamics results.
3. Since $\langle\gamma'_{\rm SR}\rangle$ is independent of orbital anisotropy, we can set a weak limit $\langle\beta_r\rangle = 0.45 \pm 0.25$ on the average anisotropy of these systems. This shows that massive galaxies are at most mildly radial anisotropic.
4. No correlation of $\gamma'_{\rm LD}$ is found with either galaxy mass or redshift, nor with radius over which this slope is measured (0.2–1.3 $R_{\rm eff}$), implying that these results are genuine and widely applicable.
5. Taking the density slope into account, an increase in luminosity is found with increasing galaxy mass, $M_{\rm eff} \propto L_{\rm eff}^{1.363\pm0.056}$, in agreement with Bolton et al. (2008b).

Based on these numerical results, we conclude that massive ETGs with total masses $M_{\rm eff} \gtrsim 3 \times 10^{10}\,M_{\odot}$ are structurally and dynamically very similar in their inner regions (roughly one effective radius), over a look-back time of about 4 Gyr, with stellar and dark-matter adding up to a combined close to isothermal density profile but having some, although relatively little, intrinsic scatter between their logarithmic density slopes. This *bulge-halo conspiracy* occurs despite (1) a clear increase in their total M/L inside one effective radius with galaxy mass (as found in this paper and in Bolton et al. 2008b), leading to a tilt in the FP, and (2) a very complex hierarchical formation history. Moreover, from the agreement between two different determinations of their average density slope—one dependent on dynamics and the other not—we also find that these galaxies are also at most mildly radially anisotropy. Our results are based on single-component mass models, which provide a good description of the available data for systems. In forthcoming publications, we will address two-component models where stellar and dark matter are modeled separately.

Our results on the near homology, isothermality, and isotropy of massive ETGs provide new constraints on theoretical models and numerical simulations of the formation of ETGs, their subsequent evolution, and the understanding of the FP. Whereas these models/simulations should match these scaling relations, they should also match their intrinsic scatter.

L.K. is supported through an NWO-VIDI program subsidy. T.T. acknowledges support from the NSF through CAREER award, by the Sloan and Packard Foundations. The work of LAM was carried out at JPL/Caltech, under a contract with NASA. Support for HST programs 10174, 10587, 10886, 10494, 10798, and 11202 was provided by NASA through a grant from the STScI.

REFERENCES

Auger, M. W. 2008, MNRAS, 383, L40
Barnabè, M., Czoske, O., Koopmans, L., Treu, T., Bolton, A., & Gavazzi, R. 2009, arXiv:0904.3861
Barnabè, M., Nipoti, C., Koopmans, L. V. E., Vegetti, S., & Ciotti, L. 2009, MNRAS, 393, 1114
Bertin, G., Ciotti, L., & Del Principe, M. 2002, A&A, 386, 149
Bolton, A. S., Burles, S., Koopmans, L. V. E., Treu, T., Gavazzi, R., Moustakas, L. A., Wayth, R., & Schlegel, D. J. 2008a, ApJ, 682, 964
Bolton, A. S., Burles, S., Koopmans, L. V. E., Treu, T., & Moustakas, L. A. 2006, ApJ, 638, 703
Bolton, A. S., Burles, S., Treu, T., Koopmans, L. V. E., & Moustakas, L. A. 2007, ApJ, 665, L105
Bolton, A. S., Treu, T., Koopmans, L. V. E., Gavazzi, R., Moustakas, L. A., Burles, S., Schlegel, D. J., & Wayth, R. 2008b, ApJ, 684, 248
Bower, R. G., Lucey, J. R., & Ellis, R. S. 1992, MNRAS, 254, 601
Cappellari, M., et al. 2006, MNRAS, 366, 1126
Czoske, O., Barnabè, M., Koopmans, L. V. E., Treu, T., & Bolton, A. S. 2008, MNRAS, 384, 987
Davis, M., Efstathiou, G., Frenk, C. S., & White, S. D. M. 1985, ApJ, 292, 371
Djorgovski, S., & Davis, M. 1987, ApJ, 313, 59
Dressler, A., Lynden-Bell, D., Burstein, D., Davies, R. L., Faber, S. M., Terlevich, R., & Wegner, G. 1987, ApJ, 313, 42
Emsellem, E., et al. 2007, MNRAS, 379, 401
Ferrarese, L., & Merritt, D. 2000, ApJ, 539, L9
Frenk, C. S., White, S. D. M., Efstathiou, G., & Davis, M. 1985, Nature, 317, 595
Gavazzi, R., Treu, T., Rhodes, J. D., Koopmans, L. V. E., Bolton, A. S., Burles, S., Massey, R. J., & Moustakas, L. A. 2007, ApJ, 667, 176
Gebhardt, K., et al. 2000, ApJ, 539, L13
Gerhard, O., Jeske, G., Saglia, R. P., & Bender, R. 1998, MNRAS, 295, 197
Gerhard, O., Kronawitter, A., Saglia, R. P., & Bender, R. 2001, AJ, 121, 1936
Gerhard, O. E. 1993, MNRAS, 265, 213
Graves, G. J., Faber, S. M., & Schiavon, R. P. 2009, ApJ, 698, 1590
Guimarães, A. C. C., & Sodré, L. J. 2009, arXiv:0904.4381
Hernquist, L. 1990, ApJ, 356, 359
Hjorth, J., & Madsen, J. 1995, ApJ, 445, 55
Hyde, J. B., & Bernardi, M. 2009, MNRAS, 396, 1171
Jaffe, W. 1983, MNRAS, 202, 995
Jiang, G., & Kochanek, C. S. 2007, ApJ, 671, 1568
Kochanek, C. S. 1991, ApJ, 373, 354
Koopmans, L. V. E., & Treu, T. 2003, ApJ, 583, 606
Koopmans, L. V. E., Treu, T., Bolton, A. S., Burles, S., & Moustakas, L. A. 2006, ApJ, 649, 599
Kormendy, J., & Richstone, D. 1995, ARA&A, 33, 581
Łokas, E. L., & Mamon, G. A. 2003, MNRAS, 343, 401
Magorrian, J., et al. 1998, AJ, 115, 2285
Mandelbaum, R., van deVen, G., & Keeton, C. R. 2009, MNRAS, in press
Nipoti, C., Londrillo, P., & Ciotti, L. 2006, MNRAS, 370, 681
Prugniel, P., & Simien, F. 1997, A&A, 321, 111
Renzini, A., & Ciotti, L. 1993, ApJ, 416, L49
Rusin, D., & Kochanek, C. S. 2005, ApJ, 623, 666
Sandage, A., & Visvanathan, N. 1978, ApJ, 223, 707
Treu, T., Gavazzi, R., Gorecki, A., Marshall, P. J., Koopmans, L. V. E., Bolton, A. S., Moustakas, L. A., & Burles, S. 2009, ApJ, 690, 670
Treu, T., & Koopmans, L. V. E. 2002, ApJ, 575, 87
Treu, T., & Koopmans, L. V. E. 2004, ApJ, 611, 739
Treu, T., Koopmans, L. V. E., Bolton, A. S., Burles, S., & Moustakas, L. A. 2006, ApJ, 650, 1219
Treu, T., Stiavelli, M., Casertano, S., Møller, P., & Bertin, G. 1999, MNRAS, 308, 1037
Visvanathan, N., & Sandage, A. 1977, ApJ, 216, 214
White, S. D. M., & Frenk, C. S. 1991, ApJ, 379, 52